

# Modeling, Simulation, and Machine Learning in Thermally Conductive Epoxy Materials



Md Rahinul Hasan Mazumder, Premika Govindaraj, Lalson D. Mathews, Nisa Salim, Dennis Antiohos, and Nishar Hameed

**Abstract** In this chapter, modeling, simulation, and machine learning methodologies are discussed to design and predict the thermal conductivity of epoxy materials. Although epoxy has some excellent properties such as chemical resistance, high tensile, compression, and bending strengths, they have relatively low thermal conductivity ( $<0.1$  W/m K). Therefore, it is ideal for designing epoxy-based composites with higher thermal conductivity for heat dissipation (TC) ( $1\text{--}10$  W/m K). Here, recent progress in the field of modeling, simulation, and machine learning is explained, describing methods of predicting the TC of epoxy materials based on different factors. Several classical theoretical models are discussed here based on their applications on the TC of epoxy-based composites. Some examples of simulation studies of the micro- and macro-scale level on the TC of epoxy-based materials are elaborated to show how these studies can be carried out to predict the TC. Finally, an overview of two different ML techniques (transfer learning and deep learning) for predicting the TC of epoxy materials is explained.

## 1 Introduction

Due to the increased demand for high-speed processors with improved efficiency in the last several years, the electronic industry is leaning toward manufacturing miniaturized and integrated devices to meet the requirements. However, it poses severe problems due to the heat accumulation in the denser assemblies of electronic devices, which might degrade their performance or might cause premature failure [1]. To overcome this challenge, thermal management materials of superior thermal conductivity (TC) and low coefficient of thermal expansion (CTE) can dissipate the heat quickly and relieve the thermal stress in these devices. Epoxies are widely used for electronic packaging due to their lightweight, excellent adhesive strength, long service life, ease of manufacturability, and excellent moisture/corrosion resistance [2, 3]. Although pure epoxy possesses a low CTE of  $50\text{--}90 \times 10^{-6} K^{-1}$  [4], its TC

---

M. R. H. Mazumder · P. Govindaraj · L. D. Mathews · N. Salim · D. Antiohos · N. Hameed (✉)  
School of Engineering, Swinburne University of Technology, Hawthorn, VIC 3122, Australia  
e-mail: [nisharhameed@swin.edu.au](mailto:nisharhameed@swin.edu.au)

is relatively low ( $\sim 0.2 \text{ Wm}^{-1} \text{ K}^{-1}$ ) [5] to be used as thermal management materials. Therefore, research has been conducted in the past years on incorporating high thermal conductive fillers into the epoxy matrix to prepare epoxy-based materials or composites with superior thermal conductivity. The traditional thermally conductive epoxy-based materials are prepared by the addition of one or several kinds of fillers such as graphene [6], boron nitride [7], aluminum nitride [8], silicon carbide [9], and zinc oxide [10].

The TC is one of the most important intrinsic material properties to design materials for thermal management applications. The TC of epoxy-based materials is influenced by several factors: bulk TC of the epoxy matrix, intrinsic TC of the fillers, fabrication methods, interfacial thermal resistance, filler morphology, filler loading level, and filler functionalization [11]. Due to the dependence of TC of epoxy materials on several factors, there a large combination of possible variables to design a thermally conductive material with the best property. Therefore, to reduce the number of possible experiments, modeling and simulation could be implemented to find the best candidate materials, saving time and resources. Furthermore, modeling and simulation can be used to study qualitatively or quantitatively the effect of various parameters on the TC of the materials. Also, in the case of 2D materials with atomic-scale thickness, measuring the TC experimentally can be a daunting task and does not always produce the best result [12]. Modeling and simulation approaches are needed in this scenario to verify and validate the experimental characterization of the TC of 2D materials.

Another method to provide a promising solution for fast and accurate prediction of physical properties including TC is machine learning (ML). ML can precisely portray the relationship between structure and properties including interactions which are nonlinear and complex. Different physical laws govern the structure and properties which does not provide a universal relationship in traditional theory or experimental works. As ML uses data mining, it can build a proper relationship without considering the laws or principles [13]. Several studies have been carried out in recent years in applying ML techniques to discover materials with desirable thermal properties. These studies considered either the atomic/molecular scope or the macroscopic physical properties [14, 15].

Figure 1 shows the different approaches to science that have progressed over time. For several hundred years, the processing and designing of materials have been carried out by experimental observation from empirical knowledge. During the twentieth century, the theoretical modeling was achieved from the extracted experimental results. With the advent of supercomputers, the theories are implemented in the simulation of complex phenomena (e.g., thermal transport phenomenon), leading to accurate predictions of the properties of materials. However, some of these scientific events are too complicated to explicitly explain with the theory. The emergence groundbreaking ML methods to teach computers the concept of those phenomena using big data sparked the “fourth paradigm of science” for materials discovery [14].

This chapter will systematically present approaches to modeling, simulation, and ML related to TC of epoxy materials. The first section will provide the fundamental theories of thermal transport in amorphous polymers such as epoxy. In the second

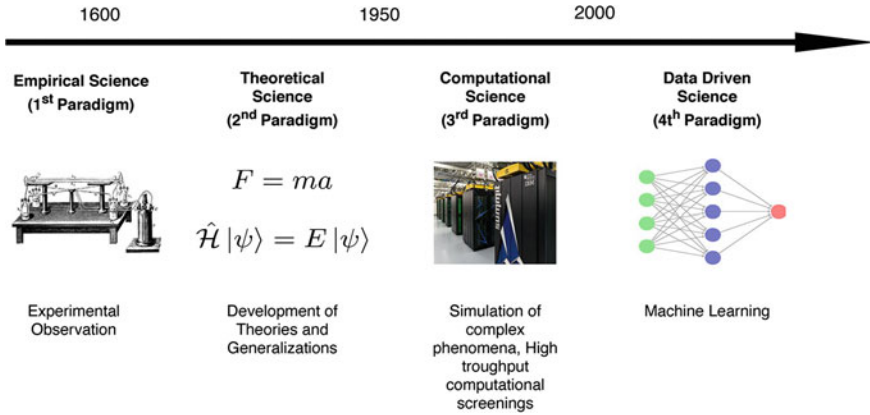


**Fig. 1** Different scientific approaches over the last four hundred years. The supercomputer image was taken from Oak ridge national laboratory [14]

section, different theoretical modeling for determining TC of epoxy composites is discussed, considering several factors such as the interaction of fillers, interfacial thermal resistance, and filler geometry. Some simulation techniques for determining the TC of epoxy materials are presented with the examples drawn from the previous simulation studies conducted on epoxy materials. Finally, ML methods for predicting the TC of epoxy materials are explained in detail with two different approaches.

## 2 Theories of Thermal Conduction in Epoxy Polymers

Thermal conduction is the principal mechanism of heat transfer in a solid material. The characteristics of thermal conduction can be expressed by the TC and specific heat capacity. The TC of solid material is expressed via Fourier’s law:

$$j_q = -\kappa \nabla T \tag{1}$$

where  $j_q$  is the heat flux ( $W/m^2$ ),  $\kappa$  is the value of TC, and  $\nabla T$  is the temperature gradient (K/m). The negative sign indicates that thermal transfer occurs down the temperature gradient. Another equation to describe the thermal conduction is the diffusive heat flow equation which is shown as

$$C \frac{\delta T}{\delta t} - \nabla(\kappa \nabla T) = \frac{\delta q_v}{\delta t} \tag{2}$$

where  $C$  is the volumetric heat capacity ( $J/Km^3$ ), and  $q_v$  is the volumetric heat flow. These two equations are the central pillar for thermal conductivity modeling by providing an analytical or numerical solution with relevant initial and boundary

conditions. However, to understand the underlying relationship between the thermal conduction and structure or bonding, the microscopic level of the material needs to be considered.

Thermal conduction occurs via heat carriers such as phonons and electrons at the microscopic level. Phonons are the main contributors of vibrational energy for thermal transport, and the resulting TC,  $\kappa$  of a bulk material can be expressed by the Debye approximation:

$$\kappa(T) = \frac{1}{3} \sum_j C_j(\omega) v_j l_j(\omega) d\omega \quad (3)$$

where  $C_j$  is the phonon specific heat with branch index  $j$  and phonon frequency  $\omega$ ,  $v_j$  is the phonon group velocity,  $l_j$  is the phonon mean free path (MFP), and  $T$  is the temperature of the bulk material [16]. However, Debye's model assumes that the vibrations are harmonic with the distribution of frequencies and high-frequency cutoff  $\omega$ , just like in a pure crystalline material. The TC increases with  $T^2$  at low temperature caused by increased specific heat, whereas at high temperature, the TC decreases linearly with  $T$  due to the Umklapp scattering of phonons.

On the other hand, epoxy polymers are amorphous or semi-crystalline materials that deviate from Debye's high-temperature model. At high temperatures, the TC of epoxy polymers reaches a plateau as  $\kappa$  increases up to a saturation point resulting from the localization of the excited phonons. This might be because the polymer materials consist of non-homogenous bonding with stiff-force constant involving the covalent bonding within the polymer backbone, and side groups coexist with softer non-bonded interactions between the chains [17–19]. Also, these non-bonded interactions are nonlinear with localized an harmonic vibrations like the “fracton hopping” model, which contributes to thermal transport [20]. Therefore, the basic thermal transport for amorphous polymers is best described by the “minimum thermal conductivity model (MTMC)” which states that the amorphous limit can be derived from Debye's model as discussed above, assuming that the lifetime of vibration is half of the period of vibrations. Considering the contribution of individual vibrations, minimum thermal conductivity,  $\kappa_{min}$  can be expressed by two measured variables (the atomic density and average sound velocity) as shown below:

$$\kappa_{min} = \left(\frac{\pi}{6}\right)^{1/3} \kappa_B n^{2/3} \sum_j^3 V_j \left(\frac{T}{\theta_j}\right)^2 \int_0^{\theta_j/T} \frac{x^3 e^x}{(e^x - 1)^2} dx \quad (4)$$

where  $\kappa_B$  is the Boltzmann constant,  $n$  is the atomic density,  $V_1 = V_l$  and  $V_{2,3} = V_t$  are the longitudinal and transverse speed of sound, respectively,  $\theta_j = V_j(\hbar/\kappa_B)(6\pi^2 n)^{1/3}$  is the Debye cutoff temperature, and  $\hbar$  is the reduced Planck constant [21]. For amorphous polymers at or above room temperature, where all vibrational modes are assumed to be thermally excited, the minimum thermal conductivity can be given

by  $\kappa_{min} = 0.40 \kappa_B n^{2/3} (V_l + 2V_f)$ . This is usually observed in polymers with long straight sections in longitudinal directions due to the drawing process.

### 3 Modeling of Thermal Conductivity of Epoxy Composites

Modeling of the TC of polymer is generally developed for their composite materials due to the low TC of the polymers. Classical theoretical modeling of TC for composites mainly falls into two types: “effective medium approximations” and “micromechanics method”. In this section, several classical models of these categories for the TC of polymer composites are explained, considering the conditions in which models can be used. The application of these models on the TC of epoxy composites is also discussed to validate the accuracy of the models in specific conditions.

#### 3.1 Rule of Mixtures and Equivalent Inclusion Models

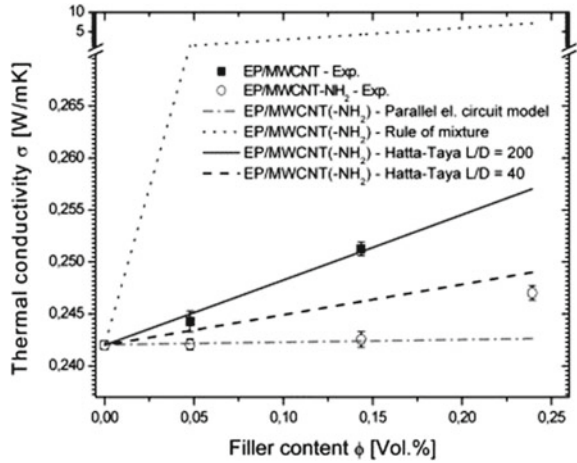
Rule of mixtures models can calculate the TC of the composites as a function of its volume fraction and the individual components’ properties. The parallel model (also known as the linear mixing rule) calculates the upper bound of the TC. In contrast, the series model (also known as the inverse mixing rule) calculates the lower bound of the TC of the composites. Most experimental results fall within these two limits in which the accuracy of the series model is greater. Assuming each component contributes independently to the overall TC of the composites and the two components are in perfect contact with each other, the series and parallel models are shown by

$$\begin{aligned} \kappa_c^{-1} &= V_f \kappa_f^{-1} + (1 - V_f) \kappa_m^{-1} \quad (\text{Series}) \\ \kappa_c &= V_f \kappa_f + (1 - V_f) \kappa_m \quad (\text{Parallel}) \end{aligned} \quad (5)$$

where  $\kappa_c$  is the TC of the composites,  $\kappa_f$  and  $\kappa_m$  are the TCs of the filler and polymer matrix, respectively, and  $V_f$  is the volume fraction of the filler [22].

To understand the mechanism involved, Gozny et al. fitted three separate theoretical models (series model, parallel model, and equivalent inclusion model) to calculate the TC of epoxy composites consisting of amino-functionalized multi-walled carbon nanotubes (MWCNT) as fillers. The correlation of the experimentally obtained TC values for MWCNT(-NH<sub>2</sub>)/epoxy composites with theoretical models is shown in Fig. 2. For the series model, they assumed that the composite was homogeneous with the fillers isolated in the matrix, which leads to TC values of the lower bound. The parallel model assumes that an internal network of conduction pathways is formed, with the fillers and matrix considered as separate phases without any interactions. This provides an overestimation of the TC values of the composites with an upper bound [23]. A third model, known as the equivalent inclusion model, which

**Fig. 2** Comparison of the TC values obtained experimentally for MWCNT(-NH<sub>2</sub>)/epoxy composites with rule of mixtures and equivalent inclusion models [23]



was developed by Hatta et al. [24] based on the previous works from Eshelby [25], was chosen to overcome the limitations of the rule of mixtures models.

The equivalent inclusion model considers the aspect ratio of the fillers, especially in a random orientation. The derived equations for the calculation of TC of 3D random short fiber-reinforced composites are shown below:

$$\frac{\kappa_c}{\kappa_m} = 1 + V_f \frac{[(\kappa_f - \kappa_m)(2S_{33} + S_{11}) + 3\kappa_m]}{J} \tag{6}$$

$$J = 3 \frac{(1 - V_f)(\kappa_f - \kappa_m)S_{11}S_{33} + \kappa_m[3(S_{11} + S_{33}) - V_f(2S_{11} + S_{33})]}{(\kappa_f - \kappa_m)} \tag{7}$$

$$S_{11} = \frac{1/D}{2[(l/D)^2 - 1]^{3/2}} \left\{ \left(\frac{l}{D}\right) \left[ \left(\frac{l}{D}\right)^2 - l \right]^{1/2} - \cosh^{-1} \left(\frac{l}{D}\right) \right\} \tag{8}$$

$$S_{33} = 1 - 2S_{11} \tag{9}$$

where  $l$  is the length of the filler and  $D$  is the diameter of the filler. From Fig. 2, it can be concluded that the obtained values from the equivalent inclusion model are in good agreement for high aspect ratio fillers with the experimental data for MWCNT/epoxy composites compared to the rule of mixtures models. However, for low aspect ratio fillers, a significant difference is observed between the experimental and fitted values, which might be due to the agglomeration of CNTs, their waviness, and the shortening of fibers during processing. In the case of amino-functionalized MWCNTs, the experimental results tend to follow the equivalent inclusion model at high filler loadings because of the increased percolation threshold due to the functionalization process [23].

### 3.2 Maxwell–Garnett (MG) Model

The Maxwell–Garnett (MG) model is one of the earliest models for predicting the TC of composites derived from the early works of Maxwell’s utilization of potential theory [26]. MG models assume that the spherical fillers are isolated within the matrix, and there is no interaction among them. At low filler loading, the theoretical values from the MG model follow a linear relationship for the TC of the composites. For a composite with no interaction between homogeneous spherical fillers randomly distributed in a homogeneous matrix, the TC is calculated by [27]:

$$\kappa_c = \kappa_m \left( 1 + 3V_f \frac{\kappa_f - \kappa_m}{2\kappa_m + \kappa_f - V_f(\kappa_f - \kappa_m)} \right) \quad (10)$$

Nayak and coworkers are used two theoretical models (rule of mixtures model and Maxwell model) and a numerical analysis model (FEM model) to compare the experimental values for TC of pine wood dust particles-reinforced epoxy composites with the predicted values. According to the Maxwell model, the fillers were spherical and dispersed, whereas the matrix was in a continuous phase. Among the two theoretical models, they found out that the deviation of the theoretical results from the experimental results is 2–44% and 4–28% for the rule of mixtures model and Maxwell model, respectively. Furthermore, they concluded from their findings that the Maxwell model overestimates the TC values, and the rule of mixtures model underestimates the TC values with respect to the experimental ones. From Fig. 3 and the results obtained, it can be stated that the Maxwell model has greater accuracy than the rule of mixtures model for a particulate filler epoxy composite. However, the Maxwell model’s accuracy is lower than the FEM model because it fails to take into account the interaction of fillers at high filler loading, and all fillers are not uniformly spherical [28].

### 3.3 Lewis-Nielsen Model

Unlike the MG model, the Lewis-Nielsen model considers the geometry and orientation of the fillers. It also considers that a thermally conductive pathway can be formed with a specific shape and size distribution of fillers at low filler loading. This model is shown as follows:

$$\kappa_c = \frac{1 + ABV_f}{1 - B\psi V_f} \quad (11)$$

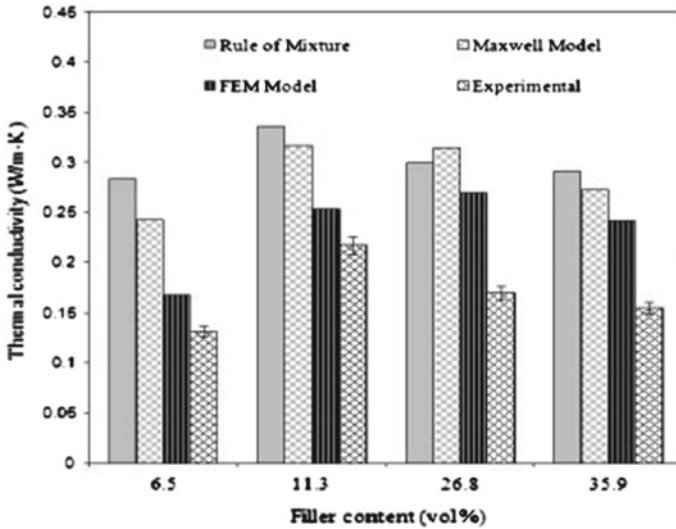


Fig. 3 Comparison of TC values obtained from the maxwell model with the other models [28]

where  $B = \frac{\kappa_f - 1}{\kappa_m + A}$  and  $\psi = 1 + \left(\frac{1 - \psi_m}{\psi_m^2}\right)f$ .  $A$  is a generalized Einstein coefficient that depends upon the filler geometry and orientation, and  $\psi_m$  is the maximum packing fraction [29].

Wang and Qiu investigated the effect of TC enhancement with incorporating CNT in glass fiber/epoxy composites through the experimental procedure and theoretical modeling with the Lewis-Nielsen model. They determined that the Lewis-Nielsen model underestimated the experimental TC values, as shown in Fig. 4. This might be because the model is invalid for fillers with a high aspect ratio, or it might have ignored entirely the orientation effect of the fillers during the processing of the composites [30].

### 3.4 Agari Model

Agari model is based on the generalization of the rule of mixtures models and considers the formation of thermal conduction chain by the interaction of fillers fraction, geometry, and the interaction between them. Therefore, the model can accurately predict the TC of composites for high filler loading [31]. Agari derived the following equation for determining TC:

$$\log \kappa_c = V_f C_2 \log \kappa_f + (1 - V_f) \log(C_1 \kappa_m) \tag{12}$$



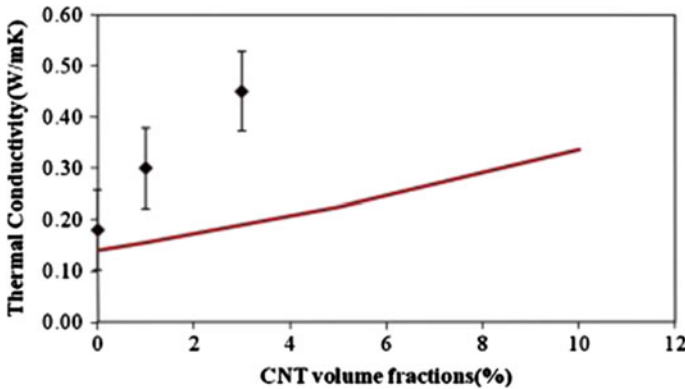


**Fig. 4** Comparison of the TC values of epoxy-CNT composites for experimental results and results obtained from the Lewis-Nielsen model (square marks: experimental results, solid line: theoretical predictions) [30]

where  $C_1$  is the correlation of the effect of the fillers on the crystallinity and crystal size of the polymer matrix, which directly influences  $\kappa_m$ , and  $C_2$  is a factor of ease in forming conducting chains of fillers and falls between 0 and 1. The value of  $C_2$  approaches 1 when particles can more easily form conductive chains, thus contributing to a greater effect to change the overall  $\kappa_c$  [32].

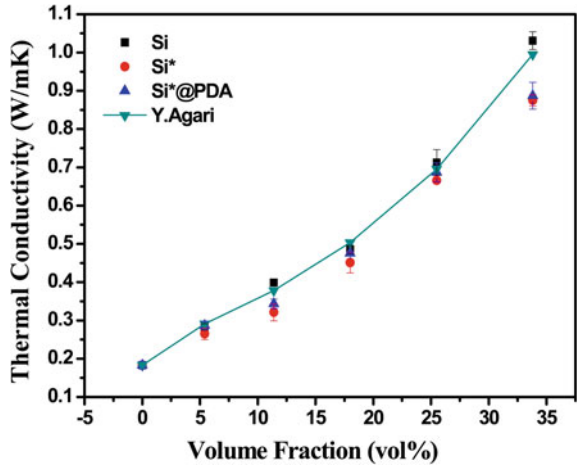
Wang and co-researchers analyzed the TC of the Si/epoxy composites by comparing the experimental data and the theoretical data from the Agari model to observe whether the model provides an accurate prediction of the TC of the composites. They reported that the predicted TC values of the composites are close to the experimental values at lower filler loading, as shown in Fig. 5. Although the model deviates at high filler loading, it should not be considered invalid because the error might be due to the poor filler dispersion and the presence of voids in the composites during the processing of the composites. Agari model does not consider these processing variables that might arise and only consider the intrinsic variables [33].

### 3.5 Bruggeman Model

The Bruggeman model considers the formation of the thermal conduction pathway due to the direct contact between the fillers. At high filler content, the distance between the fillers is small, and the fillers interact with each other. This model is an expansion of the Maxwell model as it also regards the fillers to be spherical. The Bruggeman model is defined by the following equation for a binary composite [34]:

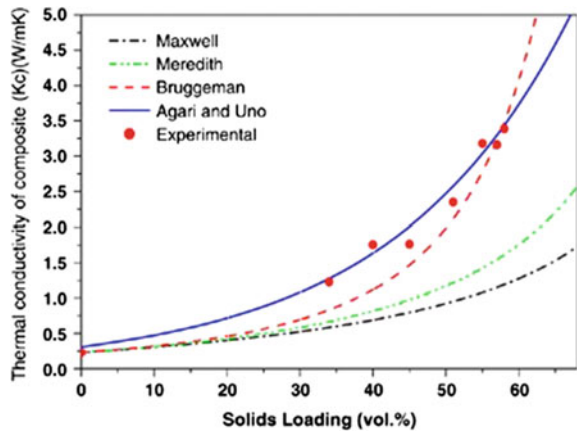
$$1 - V_f = \frac{\kappa_f - \kappa_c}{\kappa_m - \kappa_c} \left( \frac{\kappa_m}{\kappa_c} \right)^{1/3} \tag{13}$$

**Fig. 5** Comparison of the experimental and the Agari model values of the TC of the three composites with different filler volume fractions [33]



Lee and coworkers fitted several models, including the Bruggeman model, to compare how the models predict the experimental data for TC values of aluminum nitride (AlN) filled epoxy composites, as shown in Fig. 6. Bruggeman’s model provides a more accurate and consistent result at a high filler fraction than the Maxwell model as it considers the interaction among fillers. However, the Agari model matched better than the Bruggeman model as it considers the aforementioned factors,  $C_1$  and  $C_2$ , which affect the TC of the composites, unlike in the Bruggeman model, where all fillers are assumed to be spherical [35].

**Fig. 6** Comparisons of the measured TC of aluminum nitride-filled epoxy composite with the calculated TC by various theoretical models, including the Bruggeman model [35]



### 3.6 Deng-Zheng Micromechanical Model

Deng-Zheng micromechanical model does not have the limitations that other models face and thus fit perfectly for composites with low filler loading. Besides considering the effect of anisotropy, aspect ratio, and rough surfaces of the fillers, it also considers the “interfacial thermal resistance (ITR)” between the fillers or matrix and filler. The equation shows Deng-Zheng model for a 2D shaped filler-reinforced composites [36]:

$$\frac{\kappa_c}{\kappa_m} = \left[ \frac{1}{3} \frac{\eta}{\left( \frac{\kappa_m}{\eta\kappa_{ce} + H(\eta p)} \right)} \right] V_f + 1 \tag{14}$$

where  $\kappa_{ce}$  is the equivalent axial TC of the fillers as shown by the equation:

$$\kappa_{ce} = \frac{\kappa_f}{\left( 1 + \frac{2R_k\kappa_f}{L} \right)} \tag{15}$$

Here,  $R_k$  represents the Kapitza resistance, and  $L$  is the average largest lateral length of folded 2D fillers. The quantity  $H(\eta p)$  can be shown by

$$H(\eta p) = \frac{1}{((\eta p)^2 - 1)} \left[ \frac{\eta p}{\sqrt{((\eta p)^2 - 1)}} \ln \left( (\eta p) + \sqrt{((\eta p)^2 - 1)} \right) - 1 \right] \tag{16}$$

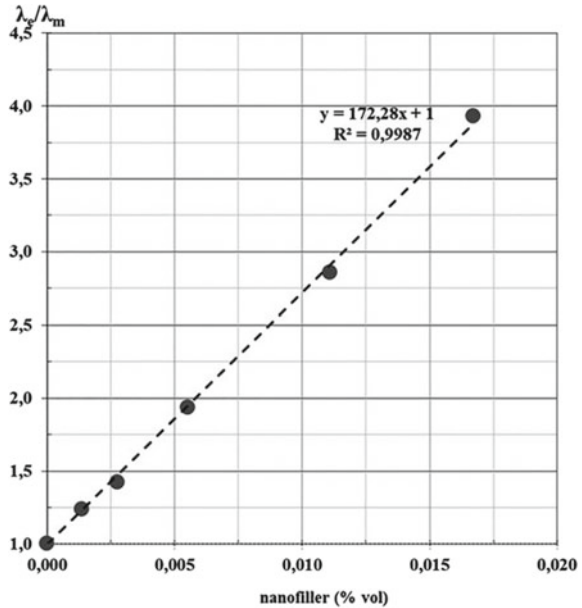
where  $p = S_A/S_L$  is the aspect ratio,  $\eta = \frac{S_A^e}{S_A}$  is the folding degree, and  $S_A^e$  is the equivalent average area of flat surface of the 2D fillers.

In Fig. 7, it is shown that the theoretical values from the Deng-Zheng model fitted perfectly with the experimental values in a straight line for epoxy composites consisting of 2D exfoliated graphene (EG) nanosheets. From the figure, the intercept and slope are calculated and found to be 1 and 172.28, respectively. The slope can also be expressed as

$$\frac{\kappa_c}{\kappa_m} = \left[ \frac{1}{3} \frac{\eta}{\left( \frac{\kappa_m}{\eta\kappa_{ce} + H(\eta p)} \right)} \right] \tag{17}$$

Putting the calculated value of the slope in the above equation, the folding degree  $\eta$  is calculated and found to be  $\eta = 0.84$ , which indicates that the fillers are not fully extended in the epoxy matrix. Therefore, Deng-Zheng’s micromechanical model also provides information on the influence of the filler’s microstructure in the matrix [37].

**Fig. 7** Experimental values (dot) and Deng-Zheng micromechanical model derived values for effective TC  $\lambda_e/\lambda_m$  of 2D EG-epoxy nanocomposites [37]



## 4 Simulation of Thermal Conductivity of Epoxy Materials

### 4.1 Molecular Dynamics Simulation

Molecular dynamics (MD) simulation is a statistical mechanics-based tool where Newton's law of motion,  $F = ma$ , is combined for a collection of particles relative to time. Using Newton's law, MD can determine the microstructure and interactions between the particles considering the particles' physical movements in a short period. In MD simulation, a force-field file is used as input to describe the physical parameters of the particles such as the atomic mass, bond angle, and bond length. The size of the MD system is typically between 10 Å and 100 nm; the number of atoms in the system is from several thousand to millions, and the simulation period is between 100 ns and microseconds [38]. MD simulations mainly fall into two categories: non-equilibrium MD (NEMD) and equilibrium MD (EMD).

The most straightforward approach for determining the TC of epoxy materials with MD simulations is the non-equilibrium molecular dynamics (NEMD) method. This method considers the arbitrary shapes and structures of the composites without any assumptions or simplifications and can describe in detail the vibrational motion of phonons. The temperature gradient is calculated by implementing heat source and sink, in which the temperatures are kept constant and then removed at a steady rate. However, it requires a large amount of computation power and time, and it also ignores the size effect of highly aligned polymer chains when the phonon mean free

path is longer than the length of aligned chains. To overcome this problem, equilibrium MD (EMD) based on Green–Kubo formalism is usually carried out. This method does not use any kind of heat source and sink and use periodic boundary conditions. Therefore, phonon scattering does not occur, and size effects are negligible. A smaller system size can be used as there is no need to establish the temperature gradient. Although the simulation time is longer, a single process can determine the whole TC tensor, which is applicable for anisotropic materials [39].

Before simulating epoxy materials, its model structures need to be generated with force acting between its atoms. Two types of molecular modeling are carried out to generate the epoxy structures: united-atom (UA) models and coarse-grained (CG) models. UA model combines a group of carbon and other heavy atoms into one particle, excluding the hydrogen atoms, and evaluates the dynamics and interaction between the particles based on united-atom force fields. As a result, it ignores most of the non-bonded interactions present in the epoxy materials. CG model treats small groups of atoms into a single particle or bead, considering all kinds of interactions and bonding energy present in the epoxy materials [38]. The non-bonded interactions are determined by pair potentials such as Lennard–Jones (LJ) potential to describe the “hard-core repulsion”, “van der Waals attraction” or “Coulomb interactions”. The bonded energies include the energy for “bond stretching”, “angle bending”, “torsion”, “inversion”, and the cross term of these functions.

#### 4.1.1 NEMD Simulation of TC of Epoxy Materials

Several studies have been carried out in recent years on NEMD simulation of TC of epoxy-based materials. Wang et al. examined the effect of incorporating functionalized graphene (FG) in epoxy resin by NEMD. At first, the equilibrated molecular structure of FG/epoxy composites is constructed by the atomistic modeling of FG and epoxy with the implementation of NVE and NPT ensemble in the MD simulation. The term “NPT ensemble” indicates that the number of atoms (N), pressure (P), and temperature (T) is kept constant during the simulation. “NVE ensemble” indicates that the number of atoms (N), volume (V), and energy (E) remains constant during the simulation. The simulation cell consists of the FG positioned in the center of the box in the XY plane direction with the epoxy chains distributed evenly on both sides of the FG, as shown in Fig. 8a. A temperature gradient is created by applying heat energy to the right side of the cell (heat source) and removing the same amount of energy from the left side (heat sink) at a constant rate. The TC of the epoxy nanocomposites is then calculated by Fourier’s law, as shown in Eq. (1). Another simulation cell is constructed to determine the TC of the nanocomposites by considering the “interfacial thermal conductance (ITC)” at the FG/epoxy interfaces. In this cell, the FG and the epoxy chains are oriented perpendicularly to the XY plane so that heat flux can pass through FG/epoxy interfaces, as shown in Fig. 8b. From the NEMD simulation, the ITC was calculated as shown by

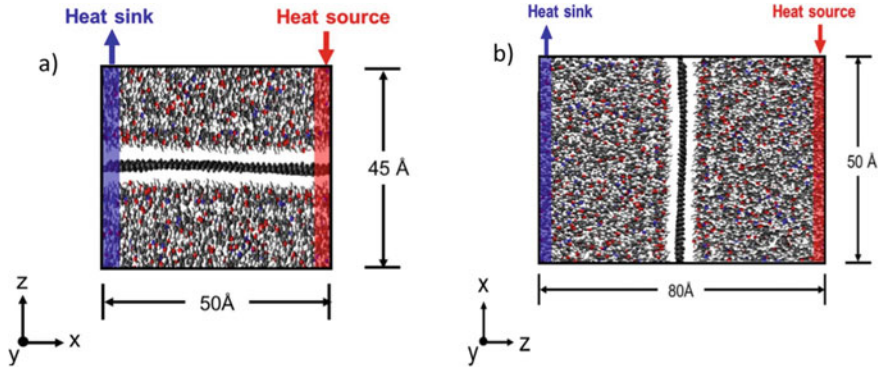


**Fig. 8** NEMD simulation for **a** in-plane TC of graphene/epoxy composite and **b** ITC of graphene/epoxy interface [40]

$$H = \frac{q}{\Delta t \cdot A \cdot \Delta T} \quad (18)$$

where  $H$  is the ITC,  $A$  is the cross-sectional area through which the heat flux passes, and  $q$  is the supplied or removed heat energy in the nanocomposite model in each step of the NVE ensemble.  $\Delta T$  is determined as the average of half of the temperature difference of the epoxy located at each side of the interface of the segmented cell regions [40].

#### 4.1.2 EMD Simulation of TC of Epoxy Materials

EMD is the most efficient way to estimate the anisotropic TC of epoxy materials at various temperatures compared to the NEMD techniques, where a single scalar quantity of TC is measured. The first step in the EMD technique is to construct the atomic modeling of epoxy polymers with sufficient cross-linking units so that their properties are portrayed properly. “Dendrimer growth approach” is the most popular method to build epoxy networks. In this technique, a single monomer of epoxy resin is modeled first, followed by cross-linking a second layer of monomers around it. The third layer of monomers is cross-linked to the second layer, and in this way, layers of monomers are added to the core structure that grows at each pass to build cubic unit cells [41]. After constructing the dendrimer structure, the TC is estimated using the “Green–Kubo expression”, which relates the TC tensor to the integral over time  $t$  of the heat flux autocorrelation function as follows:

$$\kappa = \frac{V}{3k_B T^2} \int_0^{\infty} J(0) \cdot J(t) dt \quad (19)$$

where  $V$  is the volume of the unit cell,  $\kappa_B$  is the Boltzmann's constant,  $T$  is the temperature,  $J$  is the atomistic heat flux vector, and the angular brackets denote the ensemble average, heat current autocorrelation factor,  $HCACF = J(0) \cdot J(t)$  [42].  $J$  is defined as

$$J = \sum_i e_i v_i + \frac{1}{2} \sum_{i < j} (f_{ij} (v_i + v_j)) x_{ij} \quad (20)$$

Liu et al. carried out an equilibrium MD study on the thermal and rheological properties of boron nitride nanosheets (BNNSs) filled epoxy composites. The models of neat epoxy resin and BNNS/epoxy composites were constructed using the Materials Studio 8.0 software, as shown in Fig. 9. Different force fields were used to characterize the interactions present in the model structure. CVFF potential is used for interactions between the epoxy resin and curing agent. Tersoff potential was applied to define the bonding within BNNS, and Lennard–Jones (LJ) potential was used for the interactions between epoxy and BNNS. Then, based on the “Green–Kubo theory”, EMD simulation was carried out to determine the TC of the BNNS/epoxy composites. The calculations were carried out by using the large-scale atomic/molecular massively parallel simulator (LAMMPS) package. The energy of the constructed epoxy composites system was minimized by applying the conjugate-gradient algorithm. NVT and NPT ensembles were carried out using a Nose–Hoover thermostat and barostat to accurately construct the model with the actual density. Finally, the calculations for the TC of the composites were obtained by carrying out a dynamic equilibrium for the whole model at 300 K in the atmosphere with the periodic boundary conditions applied in three directions [43].

Figure 10 shows the TC of epoxy and epoxy/BNNS composites at 300 K with the change of correlation time. The heat current autocorrelation function calculates the TC with a correlation time of 50 ps and then integrated within the correlation time interval using Eq. (20). Ten independent calculations were performed for each system to calculate its TC by averaging the TC values of the ten systems in the last 5 ps. In the figure, the thin gray line represents TC of each system, and the blue line is the average.

## 4.2 Finite Element Modeling

Finite element modeling (FEM) is a powerful numerical simulation technique to solve many engineering problems at the macroscopic level involving stress analysis, heat transfer, fluid flow, etc. Software packages such as ANSYS, ABAQUS, and COMSOL Multiphysics are general-purpose finite element modeling packages for solving wide variety of engineering problems numerically. A physical problem usually occurs in a continuum of matter (solid, liquid, or gas) with several field variables which vary from point to point in a domain resulting in an infinite number

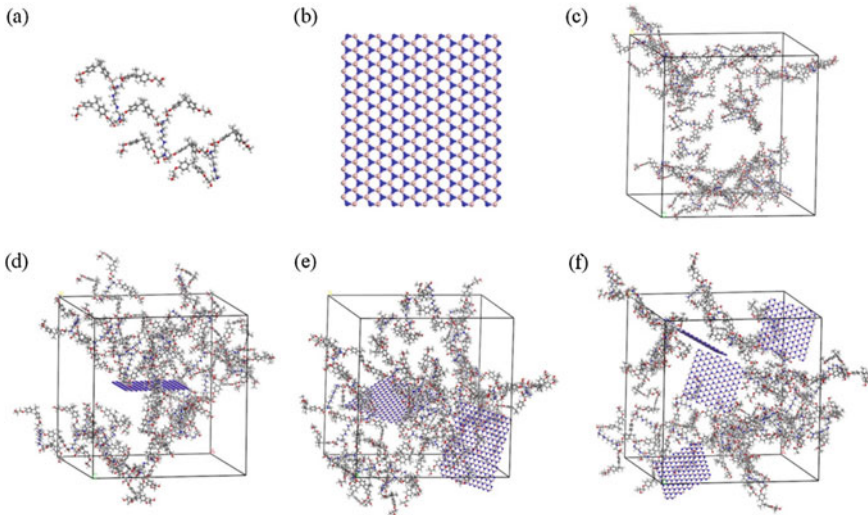


**Fig. 9** Different types of models constructed using materials studio: **a** epoxy monomer, **b** boron nitride nanosheet (BNNS), **c** neat epoxy **d–f** 10 wt.%, 2 × 10 wt.%, 4 × 5 wt.% BNNS/epoxy composites, respectively [43]

of solutions. FEM helps to provide a finite number of solutions by segmenting the domains into elements consisting of nodes located at element boundaries. These nodes reduce the physical problem by solving the variables at its locations, and the solution of these nodes can be extrapolated further from its neighboring nodes to the whole domain [25].

FEM can be used to validate and verify the values obtained from numerical simulation by comparing them with the values obtained from experimental methods or theoretical models. Recent FEM studies on determining the TC of epoxy materials mainly focused on the epoxy-based composites due to their macroscopic structure. Sharma et al. carried out FEM analysis along with experimental investigation and theoretical models to compare the TC of unfilled and marble dust-filled needle punched nanowoven jute-epoxy composites (NNPJEC).

They used ANSYS to determine the TC of the composite for different filler concentrations. A three-dimensional model of the composites was constructed in the first step by the design modeler in the ANSYS Workbench as shown in Fig. 11.  $100 \times 100 \times 100 \mu\text{m}$  cube is modeled and then segmented into alternate layers of 5 epoxy (in vol.%) and 4 jute as the reinforcing material. The marble dust particles were constructed as spherical shaped and randomly distributed in the layers of epoxy. In the next steps, the mesh parameters and boundary conditions are defined.

The geometrical model is meshed in program-controlled, linear element mode with an element size of 0.0001 mm, as shown in Fig. 12. For the boundary conditions, the temperature (T1) at nodes of face ABCD was set as 20 °C and nodes of face EFGH was set as 100 °C. The heat flow was applied in the X direction with all other sides



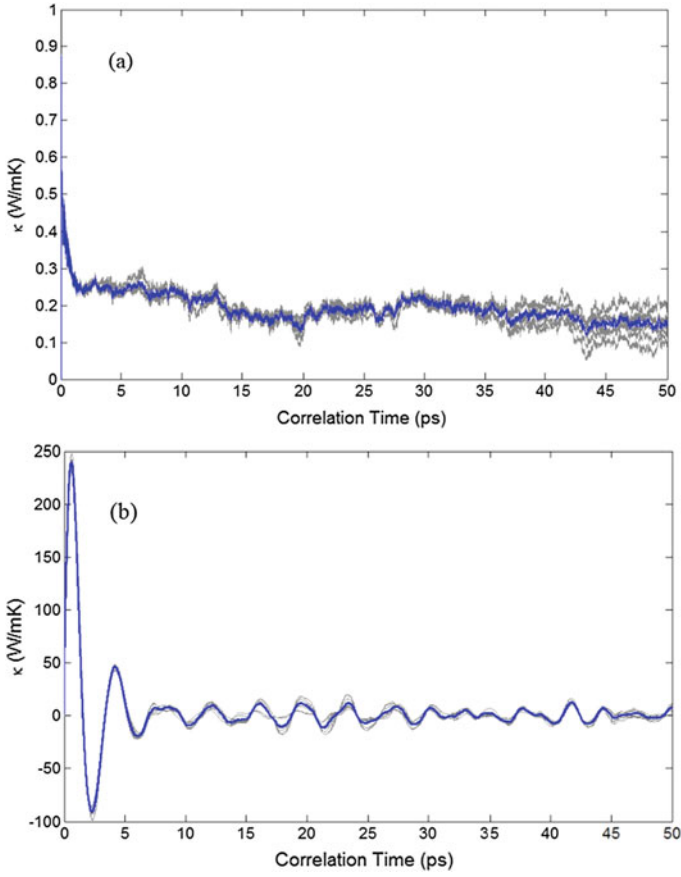


**Fig. 10** TC vs correlation time of **a** neat epoxy and **b** 10 wt.% BNNs/epoxy at 300 K [43]

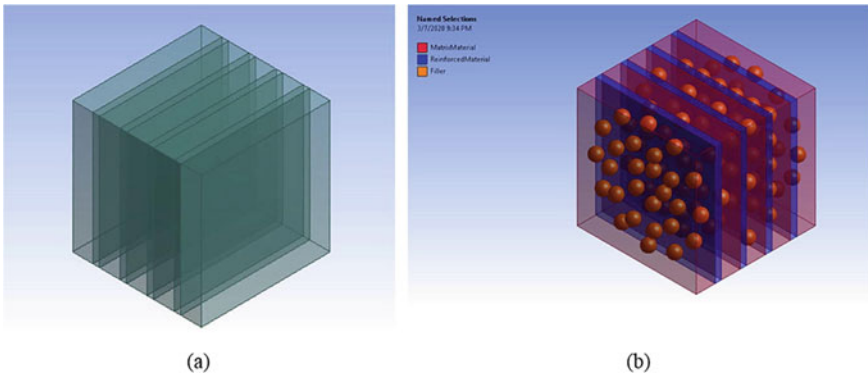


**Fig. 11** 3D geometry model for **a** unfilled and **b** MD filled NNPJEC [44]

completely insulated, as shown in Fig. 13. The numerical solution is performed using Eq. (1). The temperature distribution obtained from the simulation is shown in Fig. 14 [44].

The underlying mechanism of heat transfer in epoxy-based composites can also be understood by the FEM simulation technique. Xu and coworkers are used another simulation package for FEM called COMSOL Multiphysics 5.4 to study the heat transport and enhancement mechanism for randomly distributed BN/epoxy and 3D-BN/epoxy composites. They constructed three models of pure epoxy, randomly distributed BN (20 vol%)/epoxy, and 3D-BN (20 vol%)/epoxy with the boundary conditions defined. The temperature at the bottom is fixed at 120 °C, while the other sides are perfectly insulated with an initial temperature of 20 °C. Transient-state finite element methodology was implemented with a total time length of 0.02 s and step length of 0.002 s.

The temperature distribution and heat flux arrow of the three different models are shown in Fig. 15. The heat transfers occur evenly throughout the body of pure epoxy

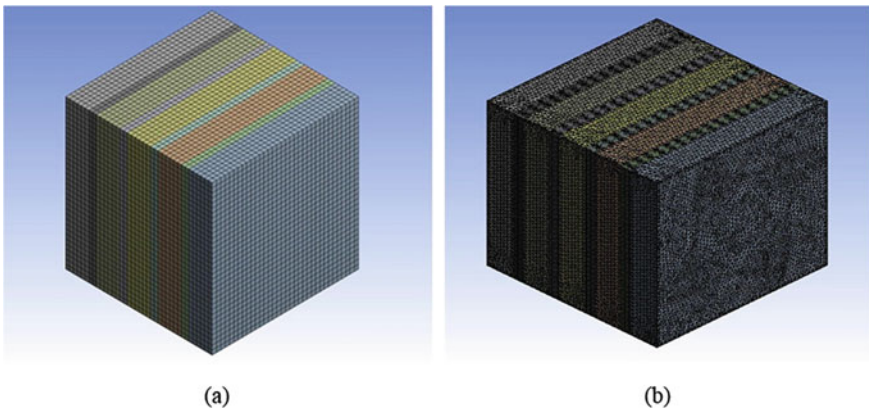
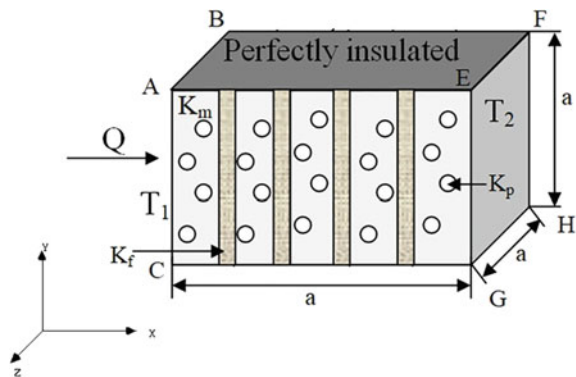
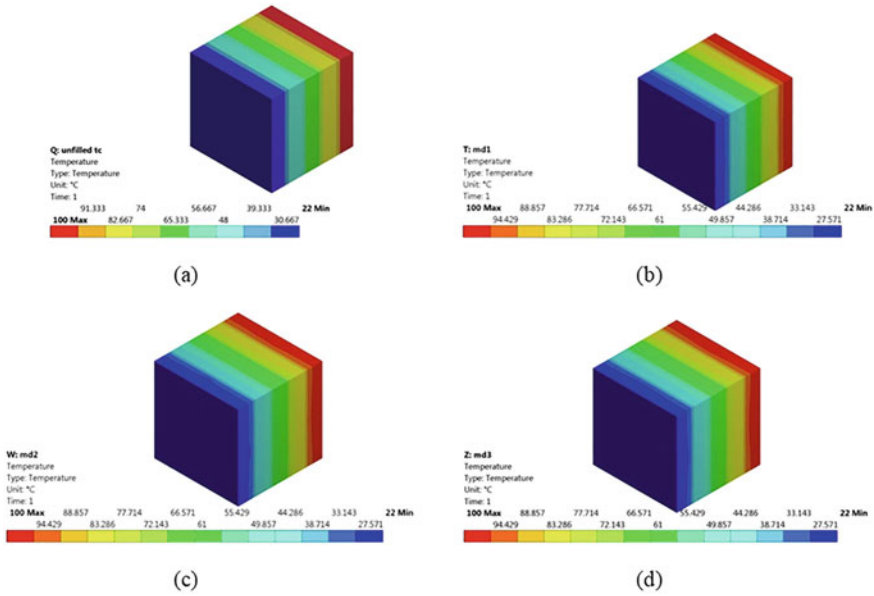


Fig. 12 Meshing for a unfilled and b MD filled NNPJEC [41]

Fig. 13 Boundary conditions for the developed model [44]





**Fig. 14** Temperature distribution profile for **a** unfilled NNPJEC and **b, c, and d** 8, 16, and 24 wt.% MD filled NNPJEC [44]

and randomly distributed BN/epoxy. The average top surface temperatures of these models remain constant throughout the whole process. This is due to insufficient thermal conduction pathway and the epoxy matrix’s low TC. On the other hand, the heat transfers faster, with the average top surface temperatures and bottom surface temperatures becoming almost equal. The 3D-BN provides selective and efficient thermal conduction pathways due to BN arrangement along the heat flow direction [45].

## 5 Machine Learning (ML) for the Thermal Conductivity of Epoxy-Based Materials

In the past few years, machine learning (ML) techniques have piqued interest in various research fields due to their excellent ability to extract useful information. ML methods can play a significant role in the design of novel materials or in predicting the physical properties of an unknown material. However, in polymer science, ML-based methods have not been widely implemented because there are not enough datasets due to the experiments being labor-intensive and expensive to construct. Furthermore, the datasets obtained from the previous literature sources are usually noisy and inconsistent because of several experimental factors such as process conditions, origin and purity of used chemicals, and environmental conditions. As a result, a

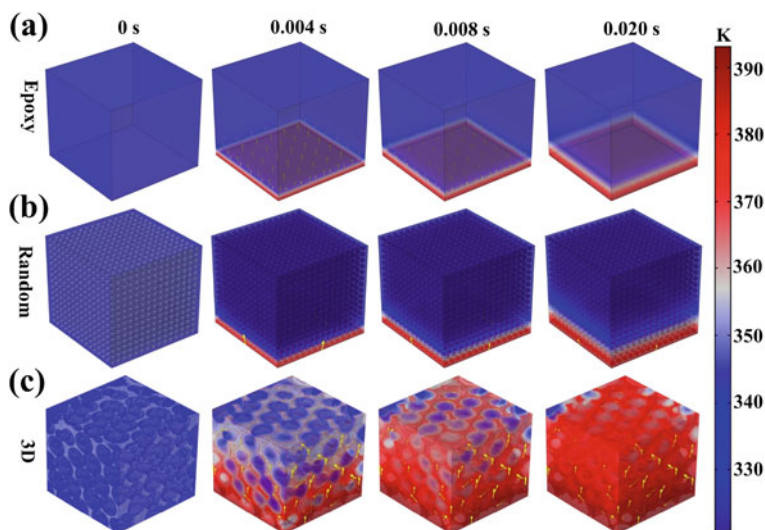


**Fig. 15** Process of heat transfer displayed by finite element simulation. Temperature distribution and heat flow arrows of **a** pure epoxy resin, **b** randomly distributed BN/epoxy composite with 20 vol% BN, **c** 3D-BN/epoxy composite with 20 vol% BN [45]

vast and comprehensible source of information on polymer properties are not easily obtainable, and the datasets are scattered [46, 47]. Moreover, for polymeric materials like epoxy, it is difficult to construct an ML model to create a link between its structure and TC. This is due to the shortage of common public databases including TC of epoxy materials. Additionally, developing an extensive database by molecular dynamics for polymers that occupy an ample chemical space is seriously limited by its longer computation time. As a second rank tensor, the obtained TC values also depend on the factors such as polymer processing operations which are not recorded in the database [48].

Few workflows have been conducted in the past to predict polymers' TC by ML methods to overcome the issue of limited data. Here, two approaches will be discussed to predict the TC of epoxy or epoxy composites materials. The first approach combines experimental techniques with active learning and Bayesian optimization to model and maximize the  $\kappa$  from various epoxy materials. This approach also helps to find out the best condition for achieving the target TC from a limited dataset without requiring any data from the previous literature through designing controlled experiments [49]. In the second approach, several ML algorithms, including "convolution neural network (CNN)", are employed to train models that can predict the effective TC of epoxy-based composites. The datasets contain composites structures that are created from a "quartet structure generation set (QSGS)", and numerical methods are applied, such as the lattice Boltzmann method (LBM), to calculate the effective TC [50]. Before discussing these approaches, an overview of the methodology of the ML framework is explained.

## 5.1 ML Methodology Framework

ML techniques generally fall into three main categories: supervised learning, unsupervised learning, and reinforcement learning. Most of the techniques used for predicting TC utilize the supervised ML strategies. Supervised learning uses the training dataset that contains a labeled set of input and output pairs for  $N$  number of samples. The goal of the supervised learning method is to evaluate a prediction  $y$  for the corresponding input  $x$  with low bias and low variance error [51]. The overall process of developing ML models consists of four steps, as shown in Fig. 16. The first step is collecting enough data from experiments, trusted numerical simulations, or other reliable sources. The second step is choosing proper features (e.g., molecular structure, physical properties, and/or chemical properties of the material) on the subject as input parameters. This is followed by capturing the effect of each parameter on the output, which leads to model training. In the last step, the final model should be evaluated by another portion of the dataset known as the testing dataset [52].

Data collection should be done so that a suitable and reliable dataset is prepared after understanding the problem and thermal transport mechanism in the material. The main objective during this process is to ensure that the training dataset represents the complete diversity of reality as much as possible. Due to the development of materials informatics in the past several years, many research groups have contributed to building databases to collect material properties for both experimental and theoretical values. These commonly used databases are Materials Project Database, Citrine Informatics, Wolfram Data Repository, Polyinfo, Cambridge Structural Database, Nanomine, and Atomwork.

Feature generation or engineering is carried out by setting up features from the training dataset that can represent both the materials in the training dataset and the new dataset. The quality of feature selection seriously influences the accuracy of the ML models. For predicting the TC of epoxy-based materials, the features might include molecular weight, specific heat capacity, density, coefficient of thermal expansion, curing temperature, curing reagent, thermal stability, etc.

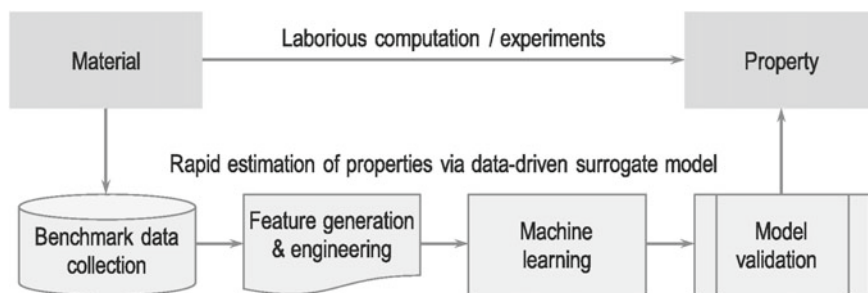


Fig. 16 Workflow for constructing a ML model for predicting TC [53]

After choosing the dataset and its features, the ML model is trained to draw a relationship between features (input data) and the TC (output data) through the ML algorithm. The complete set of data is divided into 3 sub-groups for training, validation, and testing purposes. The training data are used in the learning process by the ML algorithm to provide the ML models parameters. The validation data can optimize the hyperparameters in ML models for the best performance. To evaluate the predictive performance of the ML algorithms, three statistical performance measures are widely used: “linear correlation coefficient (R)”, “mean absolute error (MAE)”, and “root mean square error (RMSE)”. If the obtained ML model shows low accuracy to predict the TC of the testing dataset for a particular ML algorithm, the previous steps are reiterated by increasing the samples of the training dataset or choosing a different ML algorithm until the ML model shows better accuracy with the performance metrics.

## ***5.2 Prediction and Optimization of TC of Epoxy Materials from Small Dataset Through Transfer Learning***

The barrier of the limited dataset in the field of polymer science can be tackled by a two-stage data-driven approach called transfer learning. Transfer learning involves active learning and Bayesian optimization to take relevant segments of a pre-trained ML model and applying it to a new and similar problem. The objective of the first stage, active learning, is to develop a model to find epoxy materials for a specific range of high TC. Bayesian optimization is carried out in the next stage to search for epoxy materials with extremely high TC after screening the experimental conditions. It is a sample-efficient optimization method that does not require many samples to obtain good results and suitable for tasks that requires function which are extremely expensive to evaluate. The schematic for this ML-guided process including different steps is shown in Fig. 17.

At first, the data are collected from the public database such as Polyinfo and QM9 for the forward prediction step. The data for TC values had only a few instances which provide a poor accuracy for the model obtained through direct learning as shown in Fig. 19d. Therefore, an indirect approach is preferred by mapping structures of epoxy materials to proxy properties which include glass transition temperature  $T_g$ , melt temperature  $T_m$ , density  $\rho$ , and heat capacity  $C_v$ . Molecular fingerprint (ECFP) can be selected as the molecular feature to represent the chemical structure of the epoxy monomer. A linear regression model is trained on a random selection of 80% of the instances of the given data for  $T_g$  and  $T_m$ . As shown in Fig. 18c–d, the models gave decent predictions for glass transition temperature and melt temperature. Similarly, 1000 pre-trained models were constructed by using a different portion of the dataset to refine the weight parameters for the small dataset on TC values. The best transferable model to predict TC was identified from the 1000 pre-trained models that predicted the highest generalization capability on the five validation sets,

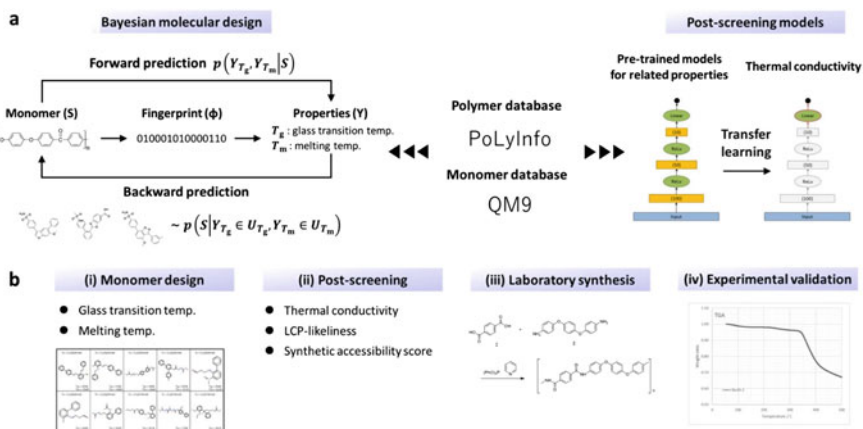


**Fig. 17** Different steps for the prediction of TC of polymers from small datasets through transfer learning. **a** Forward prediction derives a model that describes polymeric properties (e.g., glass transition temperature ( $T_g$ ) and melting temperature ( $T_m$ )) as a function of chemical structures in the constitutional repeat units. The forward model trained on the dataset from PoLyInfo was inverted to obtain a backward model, which was conditioned by desired property regions ( $U_{T_g}$  and  $U_{T_m}$ ). The backward model produced a library of hypothetical chemical structures that exhibit the desired properties. In addition, a prediction model of TC was developed, which was utilized in the post-screening of the produced library. Here, an ML framework called transfer learning was used to overcome the issue of limited data on TC: prediction models of proxy properties were pre-trained on the given large datasets from PoLyInfo and QM9, and then, the pre-trained models were fine-tuned using the limited data on the target property. The transferred model is not directly used for the molecular design calculation because its generalization capability would likely be restricted by the design space spanned by the few training polymers. **b** Analytic workflow consisting of four internal steps toward materials discovery [54]

each randomly constructed from 20% of the data. In this way, “transfer learning” is constructed to correlate TC to the molecular structure [48, 54].

However, the model is unreliable since the test dataset only has a few data points for TC. Therefore, the properties  $T_g$  and  $T_m$  are considered as design targets, whereas the transferred model is used to screen promising candidates with a high TC. Figure 18c shows the excellent accuracy of transfer learning for predicting TC. The next stage involves backward propagation for the generation of the structure of the chosen candidates. A molecular library composed of different epoxy materials is generated using the Bayesian molecular design method which requires fewer training data values. In the molecule generation process, 1000 candidates are generated based on factors such as synthetic accessibility (SA), ease of processing, validity of chemical bond, and liquid-crystalline polymers (LCPs) likeness. At the final stage, three chemical structures are selected from these 1000 candidates based on three main criteria: TC, LCPs likeness, and SA score. Finally, the monomer of these three candidates is carried out for experiments to obtain the values of the thermophysical properties for validation [48, 54].

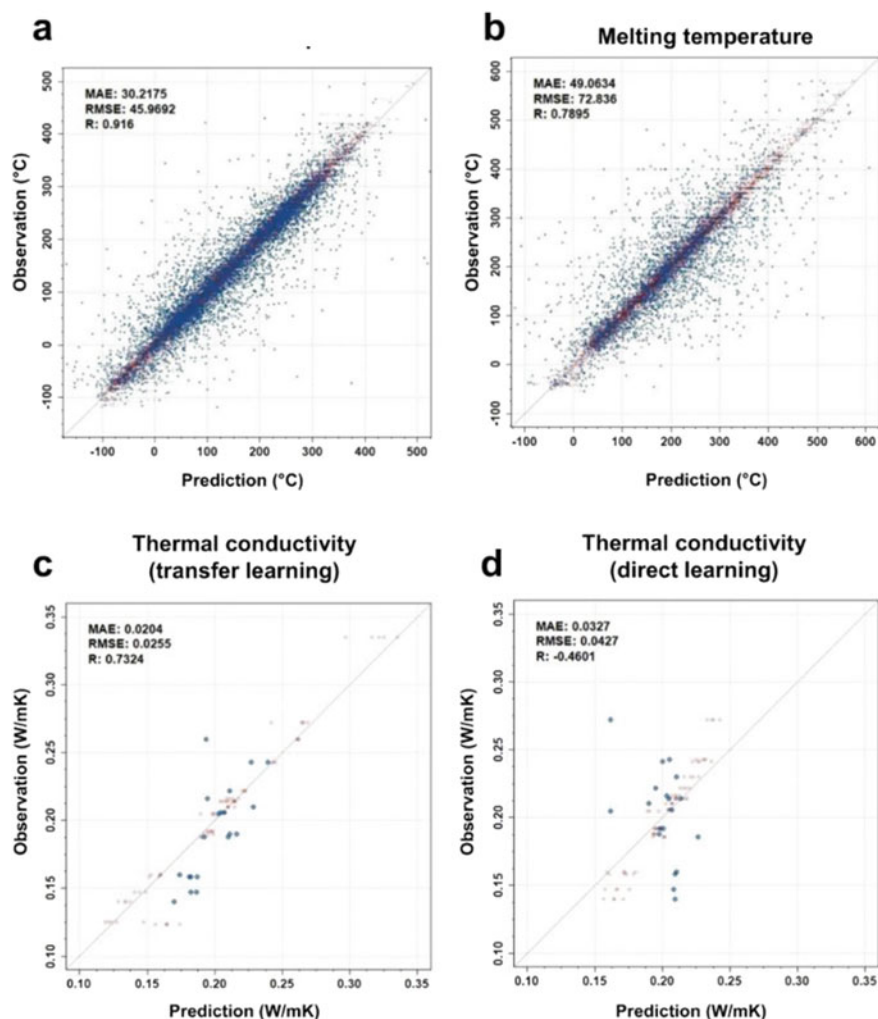


**Fig. 18** Performance of forward prediction models. **a–b** Five-fold cross-validation of trained linear models for glass transition temperature ( $T_g$ ) and melting temperature ( $T_m$ ). All predicted values in the five validation sets are plotted against observed values, denoted by blue dots (red for the training). The mean absolute error (MAE), root mean square error (RMSE), and correlation coefficient (R) are shown in each plot. **c–d** Validation results for the prediction model on TC exhibited the best transferability (MAE = 0.0204 W/mK) out of 1000 pre-trained models on  $T_m$ . The prediction results of the best-transferred model and a random forest model trained directly using the 28 data points for TC (MAE = 0.0327 W/mK) are shown in **c, d**, respectively [54]



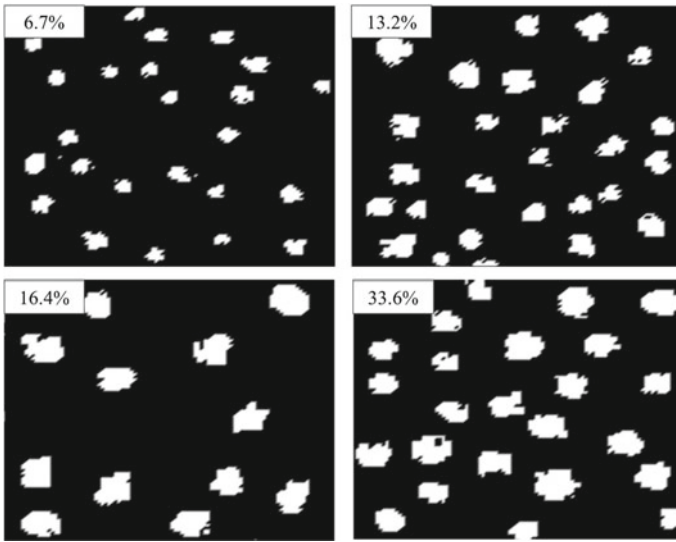


**Fig. 19** Structure of composites for different volume fractions of inclusions [50]

### 5.3 Predicting the TC of Epoxy Composites Using Deep Learning (DL) Methods

A specialized branch of ML is the deep learning (DL) which can analyze unstructured data and automated identification of features by extracting high-level features from raw input data. The use of convolution neural network (CNN) in deep learning (DL) methods of ML has been developing fast in recent years and is a handy tool for image detection. Like face recognition, CNN can also be applied to record the feature of the composites' microstructure. The extracted structural features can be used to find out the relationship between these structures and the property of the compos. CNN can provide a rapid prediction of a composite without solving tedious simulation processes or carrying out experiments.

For analyzing the heat transfer phenomenon and predicting the TC of epoxy composites, a database with different composite material structures must be constructed. The structures can be created by the quartet structure generation set (QSGS) package, and lattice Boltzmann method (LBM) is applied to calculate its effective TC. The calculated TC values obtained from LBM by solving Boltzmann transport equation (BTE) are later used in the training dataset. This method is chosen because the dataset collected from QSGS and LBM is easily obtainable. Also, the results calculated from LBM have greater accuracy as the energy from BTE follows the heat diffusion laws in macroscale composite systems. The CNN model is then applied to train the dataset to predict the effective TC of composite materials.

A large number (about 1500) of structures are generated using QSGS with different volume loading of inclusions ranging from 2 to 30%, and each volume fraction has

about 100 data. Figure 19 shows some examples of the generated structure using QSGS. The extensive training data reduce over-fitting of data and provide a model with higher accuracy. The ratio of the TC of matrix material  $\kappa_1$  and the TC of inclusion  $\kappa_2$  is fixed at a specific value (1:10) as the objective of CNN is to represent the structural features. The dataset is then divided randomly into training data and testing data. For a dataset containing 1500 structures, 1400 structures consist of training and validation data, whereas the rest of the structures are used for testing the dataset.

Several CNNs with various generated structures have been previously constructed for image recognition such as LeNet-5, AlexNet, and ResNet. Wei et al. used the LeNet-5 CNN model to predict the effective TC of composites based on their training data [50]. The architecture of this CNN model as shown in Fig. 21 is discussed here to show how the CNN model works in predicting the TC of composites from its structure. The CNN involves an input layer (i.e., the structure), an output layer (i.e., the effective TC), and multiple hidden layers. The input layer is an image of the structure with a particular pixel size (in this case  $100 \times 112$  with approx.  $10_4$  parameters). CNN reduces the number of parameters from the input to establish the mapping from the structure to the effective TC. The CNN can reduce the image to a few parameters in a one-dimensional vector using different kinds of functional layers without altering the key features of the structure, as shown in Fig. 20. Here, 96 feature maps with sizes of  $54 \times 48$  pixels containing 96 different features were obtained using the kernels of  $7 \times 7$  pixels in the first layer. The size of feature map was further reduced to  $27 \times 24$  pixels using the corresponding kernels of  $3 \times 3$  pixels in Pool-1. Using three convolution and pooling layers, the output features were converted to a one-dimensional feature vector by the fully connected layer FC-1 which in turn was processed by the fully connected layer FC-2. The feature vector is finally transformed into effective TC as the output which can be used to construct the regression model to predict the TC.

An activation function (e.g., sigmoid function) is added after each output layer to increase the nonlinearity of the network. A convolution neural kernel matrix is

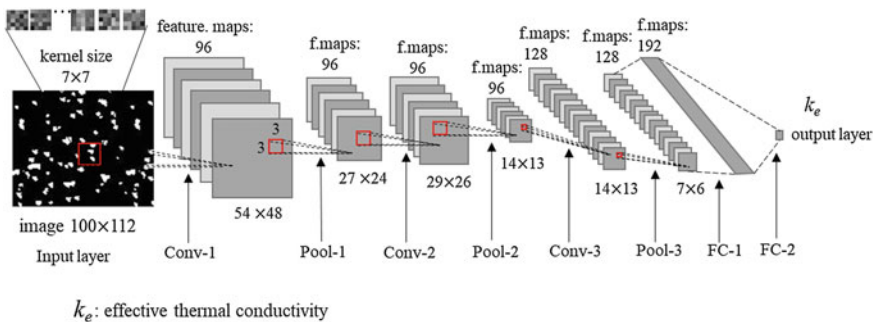
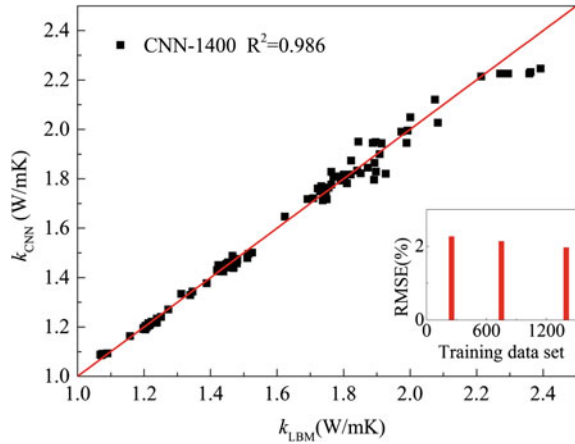


**Fig. 20** Architecture of the convolutional neural network LeNet-5. The size of kernels and the number of feature maps are indicated, and they can be adjusted according to specific needs [50]

**Fig. 21** Relationship between the TC predicted using CNN model and the LBM model. The CNN model is trained with 1400 datasets. The inset is the histogram of the RMSEs of the CNN models with different training datasets (1400, 750, 250) [50]



used for the mapping of the image of the structure to generate feature maps. The kernel parameters are first initialized by the “Gaussian initialization method” before extracting the features. Euclidean loss as the loss function is utilized for the parameters to be optimized to obtain the optimal regression model. Euclidean loss calculates the square sum of the difference between the two inputs among which one is the normalized target value, and the other is a predictive value as shown below:

$$\frac{1}{2N} \sum_{i=1}^N \|y_i - y'_i\|^2 \quad (21)$$

During the training of the neural network, the weighted parameters of the function are constantly updated according to the algorithm during each iteration to minimize the loss. After training the network, optimal parameters in the layers of the regression model are obtained which can best fit the target effective TC to the structure. From the trained CNN model, effective TC of testing data is predicted. With a testing dataset size of 100, the predicted effective TC values from the CNN model are compared with the TC values calculated by LBM. As shown in Fig. 21, the predicted results fit well with the calculated values by LBM which indicates a greater accuracy of the CNN model. It also shows that the root means square error (RMSE) decreases slightly with the number of training datasets. The RMSE is calculated by the following equation:

$$\text{RMSE} = \sqrt{\frac{1}{n} \sum_i^n \left( \frac{\kappa_{LBM-i} - \kappa_{CNN}}{\kappa_{LBM-i}} \right)^2} \quad (22)$$

where  $\kappa_{LBM}$  and  $\kappa_{CNN}$  are the calculated results from LBM and predicted results from the CNN model, respectively.

## 6 Conclusions and Future Outlook

Epoxy-based materials are widely used for thermal management applications due to their electrically insulating nature and low coefficient of thermal expansion. Highly thermally conductive fillers are usually incorporated into the epoxy matrix to develop epoxy-based materials with high thermal conductivity. Modeling and simulation are required to reduce the number of potential experiments, develop new design criteria for the selection of matrix and fillers, and understand the heat transfer mechanism for existing materials.

Over the years, various theoretical and analytical models have been developed for the prediction and description of thermal conductivity in polymer composites. These models take into consideration several assumptions such as particle size and size distribution, filler volume fraction, shape, topology, spatial distribution, and so on. For instance, the Maxwell model considers diluting dispersion of spherical particles embedded in a continuous matrix ignoring the interactions between fillers. The Bruggeman model considers filler interaction and therefore, is more accurate for high filler volume fractions. Although these models are successful in describing experimental results, the accuracy largely depends on the introduction of fitting parameters (e.g., interfacial or Kapitza resistance).

To understand the phenomenon of heat transport at the molecular level within the matrix and/or fillers through various interfaces, classical molecular dynamics (MD) simulation can be carried out. It combines the computational efficiency and the relative accuracy of the description of atomic structure, chemistry, polymer chain conformation, and bonding to determine the TC. It also considers the interfacial thermal resistance when fillers are added into the polymer matrix and accurately describes the inter-atomic forces present within the polymer matrix or fillers. Numerical simulation methods in the form of finite element modeling are another simulation technique to predict the TC of epoxy composites considering the details of materials distribution. Finite element modeling calculates the TC of the material by directly solving the heat diffusion equation through partial differential equations methods. Unlike the numerical models, it can clearly portray the heat conduction mechanism that occurs throughout the material.

ML techniques are widely used in this era of the rapid growth of technology in different fields. The development of new materials synthesis technology and the fast-growing demand for the rapid and accurate prediction of physical properties require new computational approaches like ML methods. ML methods can correlate many variables to predict the TC of an epoxy material. Also, it can be used to design a new epoxy material with the desired TC value. Here, two studies are discussed to predict the TC of epoxy materials. The first study used transfer learning to estimate its TC with limited dataset while the other study implemented DL methods to predict the TC from the microstructure of epoxy composites. However, the ML methods are relatively new and developing in the field of polymer science, and more work is needed to be done in future related to TC of epoxy materials to reach its full potential.

**Acknowledgements** Author MRM would like to acknowledge the top up scholarship from Australian Carbon Innovation. Author PG would also like to acknowledge the Swinburne University Postgraduate Research Awards research grant and thank AINSE Limited for providing financial assistance (PGRA—ALNSTU12654). NH would like to thank the Australian Research Council for the ARC DECRA (DE170101249) research grant.

## References

1. He, Z., Yan, Y., Zhang, Z.: Thermal management and temperature uniformity enhancement of electronic devices by micro heat sinks: a review. *Energy* **216**, 119223 (2021). <https://doi.org/10.1016/j.energy.2020.119223>
2. Wong, J.F., Hassan, A., Chan, J.X., Kabeb, S.M.: *Plastics in corrosion resistant applications*. Reference Module in Materials Science and Materials Engineering, Elsevier. (2020). <https://doi.org/10.1016/B978-0-12-820352-1.00072-9>
3. Hameed, N., Salim, N.V., Walsh, T.R., Wiggins, J.S., Ajayan, P.M., Fox, B.L.: Ductile thermoset polymers via controlling network flexibility. *Chem. Commun.* **51**, 9903–9906 (2015). <https://doi.org/10.1039/C4CC10192H>
4. Kim, W., Bae, J.-W., Choi, I.-D., Kim, Y.-S.: Thermally conductive EMC (epoxy molding compound) for microelectronic encapsulation. *Polym. Eng. Sci.* **39**, 756–766 (1999). <https://doi.org/10.1002/pen.11464>
5. Shimamura, A., Hotta, Y., Hyuga, H., Hotta, M., Hirao, K.: Improving the thermal conductivity of epoxy composites using a combustion-synthesized aggregated  $\beta$ - $\text{Si}_3\text{N}_4$  filler with randomly oriented grains. *Sci. Rep.* **10**, 14926 (2020). <https://doi.org/10.1038/s41598-020-71745-w>
6. Zhu, D., Qi, Y., Yu, W., Chen, L., Wang, M., Xie, H.: Enhanced thermal conductivity for graphene nanoplatelets/epoxy resin composites. *J. Therm. Sci. Eng. Appl.* **10** (2017). <https://doi.org/10.1115/1.4036796>
7. Zhang, Y., Gao, W., Li, Y., Zhao, D., Yin, H.: Hybrid fillers of hexagonal and cubic boron nitride in epoxy composites for thermal management applications. *RSC Adv.* **9**, 7388–7399 (2019). <https://doi.org/10.1039/C9RA00282K>
8. Wei, Z., Xie, W., Ge, B., Zhang, Z., Yang, W., Xia, H., et al.: Enhanced thermal conductivity of epoxy composites by constructing aluminum nitride honeycomb reinforcements. *Compos. Sci. Technol.* **199**, 108304 (2020). <https://doi.org/10.1016/j.compscitech.2020.108304>
9. Shen, D., Zhan, Z., Liu, Z., Cao, Y., Zhou, L., Liu, Y., et al.: Enhanced thermal conductivity of epoxy composites filled with silicon carbide nanowires. *Sci. Rep.* **7**, 2606 (2017). <https://doi.org/10.1038/s41598-017-02929-0>
10. Baghdadi, Y.N., Youssef, L., Bouhadir, K., Harb, M., Mustapha, S., Patra, D., et al.: The effects of modified zinc oxide nanoparticles on the mechanical/thermal properties of epoxy resin. *J. Appl. Polym. Sci.* **137**, 49330 (2020). <https://doi.org/10.1002/app.49330>
11. Guo, Y., Ruan, K., Shi, X., Yang, X., Gu, J.: Factors affecting thermal conductivities of the polymers and polymer composites: a review. *Compos. Sci. Technol.* **193**, 108134 (2020). <https://doi.org/10.1016/j.compscitech.2020.108134>
12. Sadeghi, M.M., Pettes, M.T., Shi, L.: Thermal transport in graphene. *Solid State Commun.* **152**, 1321–1330 (2012). <https://doi.org/10.1016/j.ssc.2012.04.022>
13. Wan, X., Feng, W., Wang, Y., Wang, H., Zhang, X., Deng, C., et al.: Materials discovery and properties prediction in thermal transport via materials informatics: a mini review. *Nano Lett.* **19**, 3387–3395 (2019). <https://doi.org/10.1021/acs.nanolett.8b05196>
14. Jablonka, K.M., Ongari, D., Moosavi, S.M., Smit, B.: Big-data science in porous materials: materials genomics and machine learning. *Chem. Rev.* **120**, 8066–8129 (2020). <https://doi.org/10.1021/acs.chemrev.0c00004>

15. Doblies, A., Boll, B., Fiedler, B.: Prediction of thermal exposure and mechanical behavior of epoxy resin using artificial neural networks and fourier transform infrared spectroscopy. *Polymers (Basel)* **11**, E363 (2019). <https://doi.org/10.3390/polym11020363>
16. Xu, X., Chen, J., Zhou, J., Li, B.: Thermal conductivity of polymers and their nanocomposites. *Adv. Mater.* **30**, 1705544 (2018). <https://doi.org/10.1002/adma.201705544>
17. Hsieh, W.-P., Losego, M.D., Braun, P.V., Shenogin, S., Koblinski, P., Cahill, D.G.: Testing the minimum thermal conductivity model for amorphous polymers using high pressure. *Phys. Rev. B* **83**, 174205 (2011). <https://doi.org/10.1103/PhysRevB.83.174205>
18. Wu, S., Peng, S., Hameed, N., Guo, Q., Mai, Y.-W.: A new route to nanostructured thermosets with block ionomer complexes. *Soft Matter* **8**, 688–698 (2011). <https://doi.org/10.1039/C1SM06244A>
19. Salim, N.V., Hameed, N., Fox, B.L., Hanley, T.L.: Novel approach to trigger nanostructures in thermosets using competitive hydrogen-bonding-induced phase separation (CHIPS). *Macromolecules* **48**, 8337–8345 (2015). <https://doi.org/10.1021/acs.macromol.5b00687>
20. Alexander, S., Entin-Wohlman, O., Orbach, R.: Phonon-fracton anharmonic interactions: the thermal conductivity of amorphous materials. *Phys. Rev. B* **34**, 2726–2734 (1986). <https://doi.org/10.1103/PhysRevB.34.2726>
21. Xie, X., Yang, K., Li, D., Tsai, T.-H., Shin, J., Braun, P.V., et al.: High and low thermal conductivity of amorphous macromolecules. *Phys. Rev. B* **95**, 035406 (2017). <https://doi.org/10.1103/PhysRevB.95.035406>
22. Ginzburg, V.V., Yang, J.: Modeling the thermal conductivity of polymer-inorganic nanocomposites. In: Ginzburg, V.V., Hall, L.M. (eds). *Theory and Modeling of Polymer Nanocomposites*, pp. 235–57. Cham: Springer International Publishing (2021). [https://doi.org/10.1007/978-3-030-60443-1\\_9](https://doi.org/10.1007/978-3-030-60443-1_9)
23. Gojny, F.H., Wichmann, M.H.G., Fiedler, B., Kinloch, I.A., Bauhofer, W., Windle, A.H., et al.: Evaluation and identification of electrical and thermal conduction mechanisms in carbon nanotube/epoxy composites. *Polymer* **47**, 2036–2045 (2006). <https://doi.org/10.1016/j.polymer.2006.01.029>
24. Hatta, H., Taya, M., Kulacki, F.A., Harder, J.F.: Thermal diffusivities of composites with various types of filler. *J. Compos. Mater.* **26**, 612–625 (1992). <https://doi.org/10.1177/002199839202600501>
25. Eshelby, J.D., Peierls, R.E.: The determination of the elastic field of an ellipsoidal inclusion, and related problems. *Proc. R. Soc. Lond. A* **241**, 376–396 (1957). <https://doi.org/10.1098/rspa.1957.0133>
26. Maxwell, J.C.: *A treatise on electricity and magnetism*. Clarendon Press (1873)
27. Lin, W.: Modeling of thermal conductivity of polymer nanocomposites. *Modeling and Prediction of Polymer Nanocomposite Properties*, pp. 169–200. Wiley Ltd; n.d. <https://doi.org/10.1002/9783527644346.ch8>
28. Nayak, R., Tarkes, D.P., Satapathy, A.: A computational and experimental investigation on thermal conductivity of particle reinforced epoxy composites. *Comput. Mater. Sci.* **48**, 576–581 (2010). <https://doi.org/10.1016/j.commatsci.2010.02.025>
29. Yang, X., Liang, C., Ma, T., Guo, Y., Kong, J., Gu, J., et al.: A review on thermally conductive polymeric composites: classification, measurement, model and equations, mechanism and fabrication methods. *Adv. Compos. Hybrid. Mater.* **1**, 207–230 (2018). <https://doi.org/10.1007/s42114-018-0031-8>
30. Wang, S., Qiu, J.: Enhancing thermal conductivity of glass fiber/polymer composites through carbon nanotubes incorporation. *Compos. B Eng.* **41**, 533–536 (2010). <https://doi.org/10.1016/j.compositesb.2010.07.002>
31. Zhang, H., Zhang, X., Fang, Z., Huang, Y., Xu, H., Liu, Y., et al.: Recent advances in preparation, mechanisms, and applications of thermally conductive polymer composites: a review. *J. Compos. Sci.* **4**, 180 (2020). <https://doi.org/10.3390/jcs4040180>
32. Agari, Y., Uno, T.: Estimation on thermal conductivities of filled polymers. *J. Appl. Polym. Sci.* **32**, 5705–5712 (1986). <https://doi.org/10.1002/app.1986.070320702>

33. Wang, Z., Cheng, Y., Yang, M., Huang, J., Cao, D., Chen, S., et al.: Dielectric properties and thermal conductivity of epoxy composites using core/shell structured Si/SiO<sub>2</sub>/Polydopamine. *Compos. B Eng.* **140**, 83–90 (2018). <https://doi.org/10.1016/j.compositesb.2017.12.004>
34. Bruggeman, D.A.G.: The calculation of various physical constants of heterogeneous substances. I. The dielectric constants and conductivities of mixtures composed of isotropic substances. *Ann. Phys.* **416**, 636–791 (1935)
35. Lee, E.-S., Lee, S.-M., Shanefield, D.J., Cannon, W.R.: Enhanced thermal conductivity of polymer matrix composite via high solids loading of aluminum nitride in epoxy resin. *J. Am. Ceram. Soc.* **91**, 1169–1174 (2008). <https://doi.org/10.1111/j.1551-2916.2008.02247.x>
36. Deng, F., Zheng, Q.-S., Wang, L.-F., Nan, C.-W.: Effects of anisotropy, aspect ratio, and nonstraightness of carbon nanotubes on thermal conductivity of carbon nanotube composites. *Appl. Phys. Lett.* **90**, 021914 (2007). <https://doi.org/10.1063/1.2430914>
37. Romano, V., Naddeo, C., Vertuccio, L., Lafdi, K., Guadagno, L.: Experimental evaluation and modeling of thermal conductivity of tetrafunctional epoxy resin containing different carbon nanostructures. *Polym. Eng. Sci.* **57**, 779–786 (2017). <https://doi.org/10.1002/pen.24629>
38. Zhao, J., Wu, L., Zhan, C., Shao, Q., Guo, Z., Zhang, L.: Overview of polymer nanocomposites: computer simulation understanding of physical properties. *Polymer* **133**, 272–287 (2017). <https://doi.org/10.1016/j.polymer.2017.10.035>
39. Koblinski, P.: Modeling of heat transport in polymers and their nanocomposites. In: Andreoni, W., Yip, S. (eds.) *Handbook of Materials Modeling: Applications: Current and Emerging Materials*, pp. 975–97. Cham: Springer International Publishing (2020). [https://doi.org/10.1007/978-3-319-44680-6\\_31](https://doi.org/10.1007/978-3-319-44680-6_31)
40. Wang, T.-Y., Tsai, J.-L.: Investigating thermal conductivities of functionalized graphene and graphene/epoxy nanocomposites. *Comput. Mater. Sci.* **122**, 272–280 (2016). <https://doi.org/10.1016/j.commatsci.2016.05.039>
41. Kumar, A., Sundararaghavan, V., Browning, A.: Study of temperature dependence of thermal conductivity in cross-linked epoxies using molecular dynamics simulations with long range interactions. *Model. Simul. Mater. Sci. Eng.* **22** (2014). <https://doi.org/10.1088/0965-0393/22/2/025013>
42. Kubo, R.: Statistical-mechanical theory of irreversible processes. I. General theory and simple applications to magnetic and conduction problems. *J. Phys. Soc. Jpn.* **12**, 570–86 (1957). <https://doi.org/10.1143/JPSJ.12.570>
43. Liu, Z., Li, J., Zhou, C., Zhu, W.: A molecular dynamics study on thermal and rheological properties of BNNS-epoxy nanocomposites. *Int. J. Heat Mass. Transf.* **126**, 353–362 (2018)
44. Sharma, A., Choudhary, M., Agarwal, P., Kumar Patnaik, T., Kumar Biswas, S., Patnaik, A.: Experimental and numerical investigation of thermal conductivity of marble dust filled needle punched nonwoven jute-epoxy hybrid composite. *Mater. Today: Proc.* **38**, 248–252 (2021). <https://doi.org/10.1016/j.matpr.2020.07.097>
45. Xu, X., Hu, R., Chen, M., Dong, J., Xiao, B., Wang, Q., et al.: 3D boron nitride foam filled epoxy composites with significantly enhanced thermal conductivity by a facial and scalable approach. *Chem. Eng. J.* **397**, 125447 (2020). <https://doi.org/10.1016/j.cej.2020.125447>
46. Butler, K.T., Davies, D.W., Cartwright, H., Isayev, O., Walsh, A.: Machine learning for molecular and materials science. *Nature* **559**, 547–555 (2018). <https://doi.org/10.1038/s41586-018-0337-2>
47. Jha, A., Chandrasekaran, A., Kim, C., Ramprasad, R.: Impact of dataset uncertainties on machine learning model predictions: the example of polymer glass transition temperatures. *Modell. Simul. Mater. Sci. Eng.* **27**, 024002 (2019). <https://doi.org/10.1088/1361-651X/aaf8ca>
48. Chen, G., Shen, Z., Iyer, A., Ghumman, U.F., Tang, S., Bi, J., et al.: Machine-learning-assisted De novo design of organic molecules and polymers: opportunities and challenges. *Polymers* **12**, 163 (2020). <https://doi.org/10.3390/polym12010163>
49. Pruksawan, S., Lambard, G., Samitsu, S., Sodeyama, K., Naito, M.: Prediction and optimization of epoxy adhesive strength from a small dataset through active learning. *Sci. Technol. Adv. Mater.* **20**, 1010–1021 (2019). <https://doi.org/10.1080/14686996.2019.1673670>

50. Wei, H., Zhao, S., Rong, Q., Bao, H.: Predicting the effective thermal conductivities of composite materials and porous media by machine learning methods. *Int. J. Heat Mass Transf.* **127**, 908–916 (2018). <https://doi.org/10.1016/j.ijheatmasstransfer.2018.08.082>
51. Ouyang, Y., Yu, C., Yan, G., Chen, J.: Machine learning approach for the prediction and optimization of thermal transport properties. *Front. Phys.* **16**, 43200 (2021). <https://doi.org/10.1007/s11467-020-1041-x>
52. Kwon, B., Ejaz, F., Hwang, L.K.: Machine learning for heat transfer correlations. *Int. Commun. Heat Mass. Transfer.* **116**, 104694 (2020). <https://doi.org/10.1016/j.icheatmasstransfer.2020.104694>
53. Chen, L., Tran, H., Batra, R., Kim, C., Ramprasad, R.: Machine learning models for the lattice thermal conductivity prediction of inorganic materials. *Comput. Mater. Sci.* **170**, 109155 (2019). <https://doi.org/10.1016/j.commatsci.2019.109155>
54. Wu, S., Kondo, Y., Kakimoto, M., Yang, B., Yamada, H., Kuwajima, I., et al.: Machine-learning-assisted discovery of polymers with high thermal conductivity using a molecular design algorithm. *Npj. Comput. Mater.* **5**, 1–11 (2019). <https://doi.org/10.1038/s41524-019-0203-2>